ISSN 0036-0244, Russian Journal of Physical Chemistry A, 2024, Vol. 98, No. 4, pp. 707–719. © Pleiades Publishing, Ltd., 2024.
ISSN 0036-0244, Russian Journal of Physical Chemistry A, 2024. © Pleiades Publishing, Ltd., 2024.

CHEMOINFORMATICS AND COMPUTER MODELING

1,2,4-Triazol 4-Bromobenzenesulfonates: Synthesis, Characterization (IR, NMR), DFT, Enzym Activities, and Docking Study

Reşat Ustabaş[a], Fatih Çelik[b], Nevin Süleymanoğlu[c], Halil İbrahim Güler[d], Fikret Türkan[e], Ercan Oğuz[f], and Yasemin Ünver[b,*]

[a]*Department of Mathematics and Science Education, Educational Faculty, Ondokuz Mayıs University, Kurupelit, Samsun, 55139 Turkey*

[b]*Department of Chemistry, Faculty of Sciences, Karadeniz Technical University, Trabzon, 61080 Turkey*

[c]*Graduate School of Natural and Applied Sciences, Advanced Technologies, Gazi University, Ankara, 06500 Turkey*

[d]*Department of Molecular Biology and Genetics, Karadeniz Technical University Faculty of Science, Trabzon, 61080 Turkey*

[e]*Iğdır University, Faculty of Dentistry, Department of Basic Sciences, Iğdır, 76000 Turkey*

[f]*Health Services Vocational School, Igdır University, Igdır, 76000 Turkey*

**e-mail: unver.yasemincan@hotmail.com*

Received July 19, 2023; revised October 24, 2023; accepted October 27, 2023

Abstract—(E)-4-(((3-Methyl-5-oxo-1,5-dihydro-4H-1,2,4-triazol-4-yl) imino) methyl) phenyl 4-bromo benzene sulfonate (I) and (E)-4-(((3-benzyl-5-oxo-1,5-dihydro-4H-1,2,4-triazol-4-yl) imino) methyl) phenyl 4-bromo benzene sulfonate(II) were prepared and characterized by FTIR and NMR spectroscopic methods. Density functional theory (DFT) method with 6-311++G(*d,p*) basis set was used for the theoretical study of compounds I and II. Optimized molecular structures and spectral parameters were obtained for compounds. Theoretical spectral data were compared with experimental ones and the presence of intermolecular hydrogen bonds was evaluated. Results show that in the molecular structure of compounds are available N–H···O type strong intermolucular hydrogen bonds. In this study, the inhibition effects of compounds I, II on AChE and GST enzymes were investigated. While AChE enzyme inhibitors are used in the treatment of Alzheimer's disease, GST enzyme inhibitors can be used as anti-cancer drugs. Tacrine and ethacrynic acid were studied that widely used in the international arena, as standard inhibitors. As a result, we can say that the molecules we used in the study for the gst enzyme are good inhibitors. In silico analysis was performed to investigate the possible interactions between the synthesized compounds I, II and the receptor protein.

Keywords: 1,2,4-triazol, 4-bromobenzenesulfonates, IR and NMR spectroscopy, DFT study, AChE and GST enzymes activities, docking study

DOI: 10.1134/S0036024424040204

INTRODUCTION

Sulfonates are the most commonly used leaving groups because of their ease of preparation, good nucleophilic properties, and favorable reaction rates. They also played an important role in the development of many fundamental concepts on which modern chemistry is based, such as reactions of sulfonate esters, neighboring group incorporation, solvent effects on reactivity, reaction mechanisms, non-classical carbocations, and linear free energy relationships [1]. Sulfonation is the addition of sulfonic acid groups to molecules [2] under appropriate reaction conditions. It was observed that the water solubility of the molecules obtained at the end of sulfonation increased. It has been determined that molecules containing sulfate groups show higher activities in the cell [3, 4]. These derivatives have higher antitumor, anticoagulant and antibacterial activity [5–8].

Heterocyclic compounds has been used to develop important molecules [9, 10]. The design of nitrogen-containing heterocyclic compounds is also of great interest. Most heterocyclic compounds have significant biological activities, many practical uses [11], particularly recently considered for the development of new corrosion inhibitors [12]. Azoles which are heterocyclic compounds are one of the most important nitrogen-containing structures exhibiting various biological properties. Various triazole analogs have shown pharmacological activities such as antimicrobial [13–15], antimalarial [16], antitumor [17], antifungal, antitubercular [18, 19], anti-inflammatory [20], antihistamine [21], analgesic [22], antidepressant [23], antiepileptic [24], antihypertensive [25], and antiviral [26].

Moreover, triazole derivatives are promising agents for the treatment of Alzheimer's disease [27]. Many triazole derivatives are used, such as the antibiotic Cefatrizine, the anti-HIV agent TSAO, the anticancer agent CAI, and the antibacterial agent Tazobactum [28].

Acetylcholinesterase (AChE) is a nonspecific enzyme that hydrolyzes acetylcholine, which is free or in combination with phospholipids, has a lipotrophic effect in tissues. Acetylcholine is a neurotransmitter in the central nervous system that provides communication between the brain and cells. Its deficiency causes regression in memory and cognitive functions. The release of acetylcholine from neurons stimulates striated muscles and causes them to contract [29]. Choline, which stands out in vital functions of the body, plays an active role from the inside out. In addition, it is effective in cell formation, the functioning of the nervous and muscular system, and intercellular communication. It also ensures the correct functioning of the metabolism and regulates the heartbeat [30].The brain contains neurons that contain acetylcholine. In the hippocampus part of the brain, it is responsible for forming new memories. Lack of acetylcholine in the brain causes Alzheimer's disease (AD). For this reason, it is of great importance in the brain in terms of memory and not forgetting memories. Inhibitors of cholinesterase enzymes can also be used as drugs in the treatment of AD disease [31].

Glutathione-S-transferase (GST) is a multifunctional enzyme that provides internal balance by catalyzing the first step of mercapturic acid formation in detoxification metabolism. GST shows antioxidant properties in terms of eliminating toxic substances taken with food [32]. Glutathione S-transferases are a multifunctional enzyme that has an important role in xenobiotic metabolism. Therefore, the decrease in GST enzyme activity causes a decrease in the detoxification ability of the liver. Inhibitors of this enzyme can be recommended as drugs in the treatment of damaged tissues [33, 34].

In this study; (E)-4-(((3-methyl-5-oxo-1,5-dihydro-4H-1,2,4-triazol-4-yl)imino) methyl) phenyl 4-bromobenzenesulfonate (I) and (E)-4-(((3-benzyl-5-oxo-1,5-dihydro-4H-1,2,4-triazol-4-yl) imino) methyl) phenyl 4-bromo benzene sulfonate (II) were synthesized and characterized by FTIR and NMR spectroscopic methods. The theoretical study was carried out by density functional theory (DFT) method with 6-311++G(*d,p*) basis set. the inhibition effects of compounds I, II on AChE and GST enzymes were investigated. While AChE enzyme inhibitors are used in the treatment of Alzheimer's disease, GST enzyme inhibitors can be used as anti-cancer drugs. In silico analysis was performed to investigate the possible interactions between the synthesized compounds I, II and the receptor protein.

RESULTS AND DISCUSSION

Synthesis

When the IR spectra of compounds I, II were examined, the vibrational bands of the carbonyl (C=O) and amine (NH_2) groups of the starting compounds were not observed in the IR spectra. The ^{1}H-NMR data of the imine group formed as a result of the reaction of aldehyde and amine appeared as 9.72 and 9.68 ppm of compounds I, II respectively. ^{13}C NMR peaks of this group (CH=N) were observed at 152.38 and 152.14 ppm. NH protons of the triazole ring for compounds I, II appeared at 11.84 and 12.00 ppm as singlet respectively. Carbon peaks of the C=N group in the triazole ring were observed at 150.95 ppm for both compounds. Both proton and carbon peaks of aromatic rings were seen in the expected regions.

Geometry Optimizations

Compound I has two benzene rings and one triazole ring in its molecular structure. In the molecular structure of compound II, unlike compound I, CH_2–benzene ring is bonded to the C23 atom in the triazole ring. The optimization of both structures was completed using the DFT/B3LYP/6-311G++(*d,p*) method. Structural parameters resulting from the optimization can be found in Table 1 and molecular images of both molecules can be found in Fig. 1. When comparing the structural parameters of both optimized structures, the focus was on the inductive effect of compound II on the structural parameters of the trizazole ring of the CH2-benzene ring bonded from the C23 atom.

The bond lengths of C23–N25, N25–C24, C24–N30, N30–N29, N29=C23 and C23–C31 in the triazole rings of compounds I and II are 1.400/1.402, 1.423/1.420, 1.373/1.373, 1.375/1.374, 1.297/1.296, and 1.490/1.504 Å, respectively. The bond angles of C31–C23–N25 and C31–C23–N29 are 126.6°/125.1° and 122.7°/124.2°, respectively. C36–N22–N25–C23 and N22–N25–C23–C31 torsion angles of compounds I and II are –37.24°/–44.22° and 5.39°/7.03°, respectively. The dihedral angles between two phenyl (Bz1: C1–C6; Bz2: C11–C16) and triazole rings (Tr: N25, C24, N30, N29, C23) in the structure of compounds I and II are Bz1/Bz2 = 35.87°/26.81°, Bz1/Tr = 30.90°/52.67°, and Bz2/Tr = 30.47°/39.20°, respectively. When the above mentioned results of compounds I and II are analyzed, it is seen that the greatest inductive effect is in dihedral angles.

Since the structural parameters of compounds I and II were calculated in the gas phase, comparison was made with the structural parameters of similar structures in the solid phase (X-ray) in the literature. The bond lengths of C–Br, S=O, C=O and C=N and N–N in triazole ring in the structures of both molecules are 1.910, 1.453 and 1.455/1.454 and 1.455,

Table 1. Some optimized parameters obtained by DFT/B3LYP/6-311G++(*d,p*) method of compounds I and II

Compound I					
Bond lengths, Å					
C1–C2	1.391	S37–O39	1.455	C13–C36	1.465
C2–C3	1.392	S37–O21	1.679	C36–N22	1.280
C3–C4	1.392	O21–C16	1.399	N22–N25	1.372
C4–C5	1.391	C16–C11	1.391	N25–C24	1.423
C5–C6	1.394	C11–C12	1.391	C24–O28	1.209
C6–C1	1.394	C12–C13	1.401	C24–N30	1.373
C6–Br27	1.910	C13–C14	1.405	N30–N29	1.375
C3–S37	1.784	C14–C15	1.386	N29–C23	1.297
S37–O38	1.453	C15–C16	1.394	C23–C31	1.490
Bond angles, deg					
C1–C6–Br27	119.2	S37–O21–C16	118.5	N25–C23–C31	126.6
C5–C6–Br27	119.2	C36–N22–N25	119.3	N29–C23–C31	122.7
C3–S37–O38	110.1	N25–C24–O28	128.6	N30–C24–O28	130.3
C3–S37–O39	109.8	N22–N25–C23	132.5	C13–C36–N22	120.8
Torsion angles, deg					
C2–C3–S37–O38	–19.77	O38–S37–O21–C16	–56.87	N22–N25–C23–C31	5.39
C4–C3–S37–O39	24.60	O39–S37–O21–C16	75.68	N22–N25–C24–O28	–7.26
Compound II					
Bond lengths, Å					
C1–C2	1.391	O21–C16	1.399	C24–O28	1.209
C2–C3	1.392	C16–C11	1.390	C24–N30	1.373
C3–C4	1.392	C11–C12	1.391	N30–N29	1.374
C4–C5	1.391	C12–C13	1.401	N29–C23	1.296
C5–C6	1.394	C13–C14	1.405	C23–C31	1.504
C6–C1	1.394	C14–C15	1.386	C31–C37	1.515
C6–Br27	1.910	C15–C16	1.394	C37–C38	1.397
C3–S47	1.784	C13–C33	1.464	C38–C39	1.393
S47–O48	1.454	C33–N22	1.280	C39–C34	1.394
S47–O49	1.455	N22–N25	1.376	C34–C35	1.393
S47–O21	1.680	N25–C24	1.420	C35–C36	1.394
Bond angles, deg					
C1–C6–Br27	119.2	S47–O21–C16	117.9	N25–C23–C31	125.1
C5–C6–Br27	119.2	C33–N22–N25	118.3	N29–C23–C31	124.2
C3–S47–O48	110.1	N25–C24–O28	128.6	N30–C24–O28	130.3
C3–S47–O49	109.9	N22–N25–C23	131.9	C23–C31–C37	113.4
Torsion angles, deg					
C2–C3–S47–O48	20.89	O48–S47–O21–C16	64.23	N22–N25–C23–C31	7.03
C4–C3–S47–O49	–23.41	O49–S47–O21–C16	–68.32	N22–N25–C24–O28	–8.23

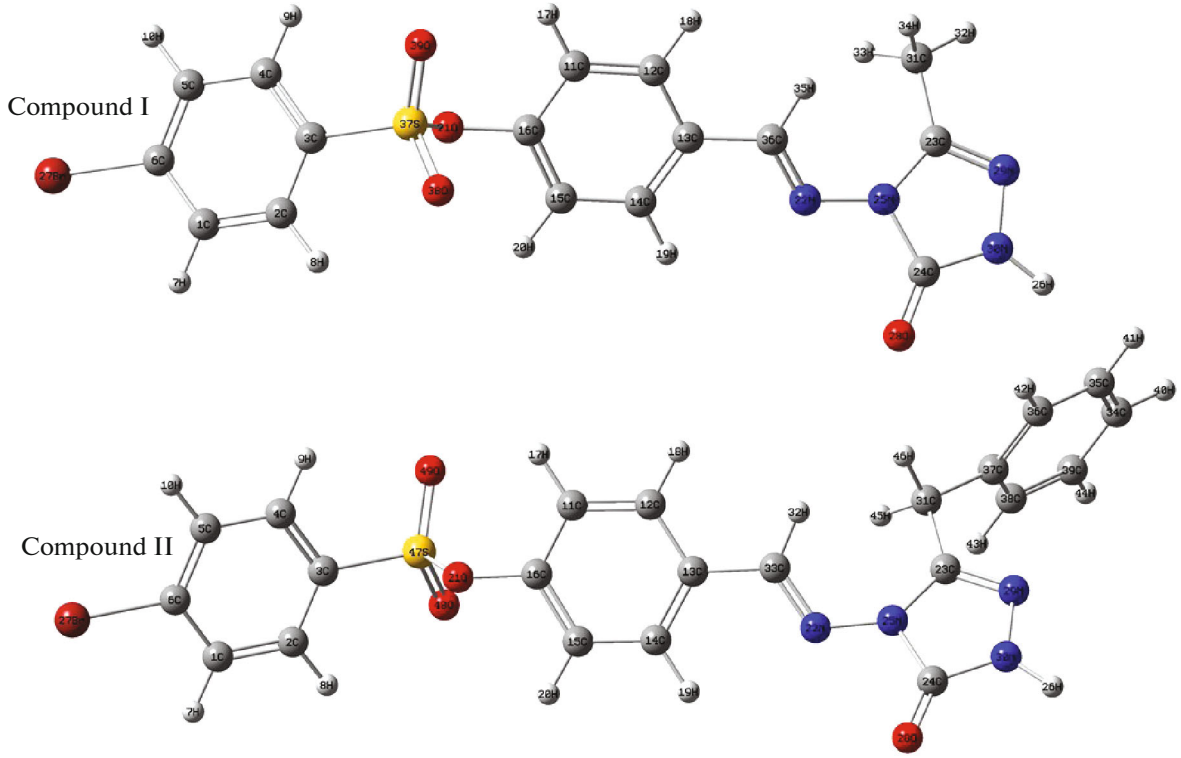

Fig. 1. The molecular structures for compounds I and II.

1.209, 1.297/1.296 and 1.375/1.374 Å, respectively. In the literature, it was found as 1.897 (2)/1.905 (7), 1.4277 (17) and 1.4239 (16)/1.427 (4) and 1.430 (4) [35, 36], 1.224 (2)/1.239 (3), 1.288 (2)/1.290 (3) and 1.372 (2)/1.389 (3) Å [37, 38]. The O–C–N bond angles of both molecules are 128.6° and 130.3°. These bond angles are 128.01 (18)°/128.20 (18)° and 128.1 (2)°/129.0 (2)° in [37, 38].

It is seen that the calculated structural parameters of compounds I and II are compatible with the structural parameters given in the literature (X-ray). The method used in the calculation of both structures and the selection of the base function show that they are correct.

Vibrational Spectra and NMR Spectra

The IR and NMR spectral data for compounds I and II were obtained at DFT/B3LYP/6-311++G(*d,p*) level and given in Tables 2 and 3 as scaled. It can be seen from Table 2 that theoretical IR data verify the molecular structures of compounds I and II very well. For compounds I and II, the N=C–H stretching bands at 1602 and 1589 cm^{-1} in FTIR spectra were obtained as 1645 and 1644 cm^{-1}, respectively. However, the N–H stretching bands at 3177 and 3169 cm^{-1} were calculated as 3529 and 3532 cm^{-1}, respectively. The difference between experimental data and theoretical ones are 352 and 363 cm^{-1}, respectively. These considerable deviations in IR data can be attributed to the presence of strong intermolecular hydrogen bonds in the molecular structures of compounds I and II. Because, DFT calculations were carried out in gas state and therefore molecular interactions were not taken into account.

As compared the theoretical and experimental NMR data given in Table 3, it can be seen that NMR spectral data are generally very compatible each other for compounds I and II. CH=N signals in ^{13}C-NMR spectra were observed as 152.35 and 152.24 ppm and obtained as 166.96 and 169.98 ppm, respectively. The CH=N signals at 9.72 and 9.68 ppm in ^{1}H-NMR spectra were calculated as 8.63 and 8.81 ppm, respectively.

However, NH signals were observed at 11.84 and 12.00 ppm and calculated as 7.94 and 7.86 ppm, respectively. The deviations for NH signals are 3.90 ppm for compound I and 4.14 ppm for compound II. Deviations from the experimental values for N–H stretching bands in theoretical IR data are also present for NH signal in the NMR data. Therefore, it can be stated that NMR data support the IR results and similarly point to strong intermolecular hydrogen bonds of N–H···O type in the molecular structure of compounds I and II.

Table 2. Some experimental and scaled theoretical vibration frequencies (cm^{-1}) of compounds I and II, obtained with DFT/B3LYP/6-311++G(*d,p*)

Assingments*	Compound I			Compound II		
	exp. IR (cm^{-1})	calculated (scaled)		exp. IR (cm^{-1})	calculated (scaled)	
		freq.	I_{IR} (km/mol)		freq.	I_{IR} (km/mol)
ν(N–H)triaz.	3177	3529	132.70	3169	3532	119.82
ν(C–H)arom	3048	3078–3034	1.85–10.59	3031	3079–3025	2.12–7.71
ν(CH3)as	2883	3001, 2961	4.89, 6.61	—	—	—
ν(CH3)s		2908	12.43	—	—	—
ν(N=C–H)	3048	2972	30.71	3031	2962	31.15
ν(CH2)as	—	—	—	2883	2930	3.75
ν(CH2)s	—	—	—		2897	25.38
ν(C=O)triaz	1698	1749	638.97	1703	1745	730.88
ν(N=C–H)	1602	1645	1.74	1589	1644	2.54
ν(N=C)triaz	1602	1609	45.24	1589	1601, 1599	32.47, 18.03
ν(C=C)	1573			1574		
ν(O=S=O)		1288	99.62		1288	120.92

* ν; stretching.

Enzym Activities

The inhibition study was carried out in two steps, IC_{50} and Ki for both enzymes. The IC_{50} values of the Acetylcholineesterase enzyme were found as 2.44–1.73 for compounds I, II, respectively. R^2 values were found to be 0.9854–0.9843. Tacrine molecule was used as the standard inhibitor and the results were compared with compounds I, II. The IC_{50} value for the tacrine molecule was 0.48 and the r^2 value was 0.9584. After the determination of the IC_{50} values, the Ki study, which is another step, was performed and the effectiveness of the inhibitor was determined by comparing it with the standard molecule. The Ki study was obtained by plotting the lineweaver burk graph and Ki values of AChE enzyme were found to be 4.1367 ± 0.597 for compound I 5.2233 ± 0.44 for compound II at micromolar concentration. The Ki value of tacrin, which was studied as a standard inhibitor, was found to be 0.8933 ± 0.0666. The inhibition values of this enzyme are shown in Table 4 and Fig. 2.

When the research findings made in recent years are examined, it is seen that molecules such as tacrine and donepezil are generally used as standard inhibitors. Our study findings seem to be compatible with [39].

When the GST enzyme innovation results were evaluated, it was seen that the IC_{50} values of the compounds I, II molecules were in the range of 2.75–1.69 and the r^2 values were in the range of 0.9568–0.9722. Ethacriynic acid, which is widely used as the standard inhibitor, was used in the study. The IC_{50} value was 3.15 and the r^2 value was 0.9985. Ki values of compounds I, II were found to be 8.1867 ± 6.5654 and 5.7967 ± 5.4957, respectively. The Ki value of the standard inhibitor was calculated as 24.257 ± 16.598. All research findings are shown in Table 4 and Fig. 3.

When the literature studies on the GST enzyme are examined, it is seen that the inhibition studies are similarly performed in the form of IC_{50} and Ki. It is seen that ethacrynic acid is similarly used in studies as a standard inhibitor. Inhibition findings at the micromolar level are consistent with [40].

Molecular Docking

Molecular docking is a computational method used in drug discovery and design to predict the binding orientation and affinity of a small molecule to a receptor target of interest. It also has become an important tool in drug discovery and design as it can accelerate the screening process and reduce the cost and time required for experimental validation [41]. In this study, two newly synthesized compounds with a wide range of biological activities were investigated by in silico analysis as a potential drug candidate against glutathione s-transferase.

Glutathione S-transferase (GST) is an enzyme that plays an important role in the detoxification of

Table 3. Experimental and theoretical ^{1}H- and ^{13}C-NMR spectra data of compounds I and II (in ppm)

Atom	Compound I		Compound II	
	exp.	calculated (in DMSO)	exp.	calculated (in DMSO)
$C_{36(I),33(II)}=N$	152.35	166.96	152.24	169.98
$C_{23}=N_{triaz}$	150.95	150.42	150.93	153.62
$C_{24}=O_{triaz}$	151.55	158.14	151.59	158.14
$(C_{1,2,3,4,5,6})_{arom}$	133.53 129.68 133.75 129.68 133.53 133.35	139.97 135.19 145.69 135.46 139.99 157.83	133.53 129.95 133.74 129.95 133.53 133.38	139.74 136.23 144.97 136.04 139.74 157.71
$(C_{11,12,13,14,15,16})_{arom}$	123.33 130.80 129.97 130.80 123.23 144.65	131.96 141.87 139.64 133.92 132.77 159.86	123.26 130.67 129.99 130.67 123.26 146.69	132.22 141.89 139.33 133.83 132.67 159.86
$(C_{34,35,36,37,38,39})_{arom}$	—	—	127.20 128.92 129.26 136.21	133.41 135.61 137.28 143.14 137.81 135.14
$(C_{31}H3)$	10.93	15.85	—	—
$(C_{31}H2)$	—	—	31.07	38.15
$(CH_{7,8,9,10})_{arom}$	7.81–7.90	7.91 8.22 8.27 8.02	7.80–7.92	8.05 8.26 8.22 8.12
$(CH_{17,18,19,20})_{arom}$	7.20 7.81–7.90 7.81–7.90 7.20	7.86 8.00 8.80 7.78	7.18–7.32 7.80–7.92 7.80–7.92 7.18–7.32	7.74 8.01 8.78 7.74
$(CH_{40,41,42,43,44})_{arom}$	—	—	7.18–7.32	7.57 7.64 7.57 7.83 7.78
$N=CH_{35(I),32(II)}$	9.72	8.63	9.68	8.81
$(NH_{26})_{triazol}$	11.84	7.94	12.00	7.86
$CH_{32,33,34}$	2.27	2.34 2.17 2.59	—	—
$CH_{45,46}$	—	—	4.05	4.18 3.80

Table 4. The effects of compounds I and II on glutathione S-transferase acetylcholinesterase enzymes activity

Compounds	IC_{50}, μM				Ki, μM	
	AChE	r^2	GST	r^2	AChE	GST
I	2.44	0.9854	2.75	0.9568	4.1367 ± 0.597	8.1867 ± 6.5654
II	1.73	0.9843	1.69	0.9722	5.2233 ± 0.44	5.7967 ± 5.4957
Tacrin	0.48	0.9584	—	—	0.8933 ± 0.0666	—
Ethacriynic acid	—	—	3.15	0.9985	—	24.257 ± 16.598

endogenous and exogenous compounds in human cells. It catalyzes the conjugation of glutathione (GSH) with a wide range of electrophilic compounds, including carcinogens, environmental toxins, and reactive oxygen species (ROS), to form less toxic and more water-soluble metabolites that can be eliminated from the body [42].

The docking results showed that compounds I, II had appreciably strong binding affinities against glutathione s-transferase. Results of molecular docking including binding energies, Ki values and interacted residues are summarized in Table 5. Compound II showed a higher docking score (–8.20 kcal/mol) with receptor protein compared to that of the other ligand

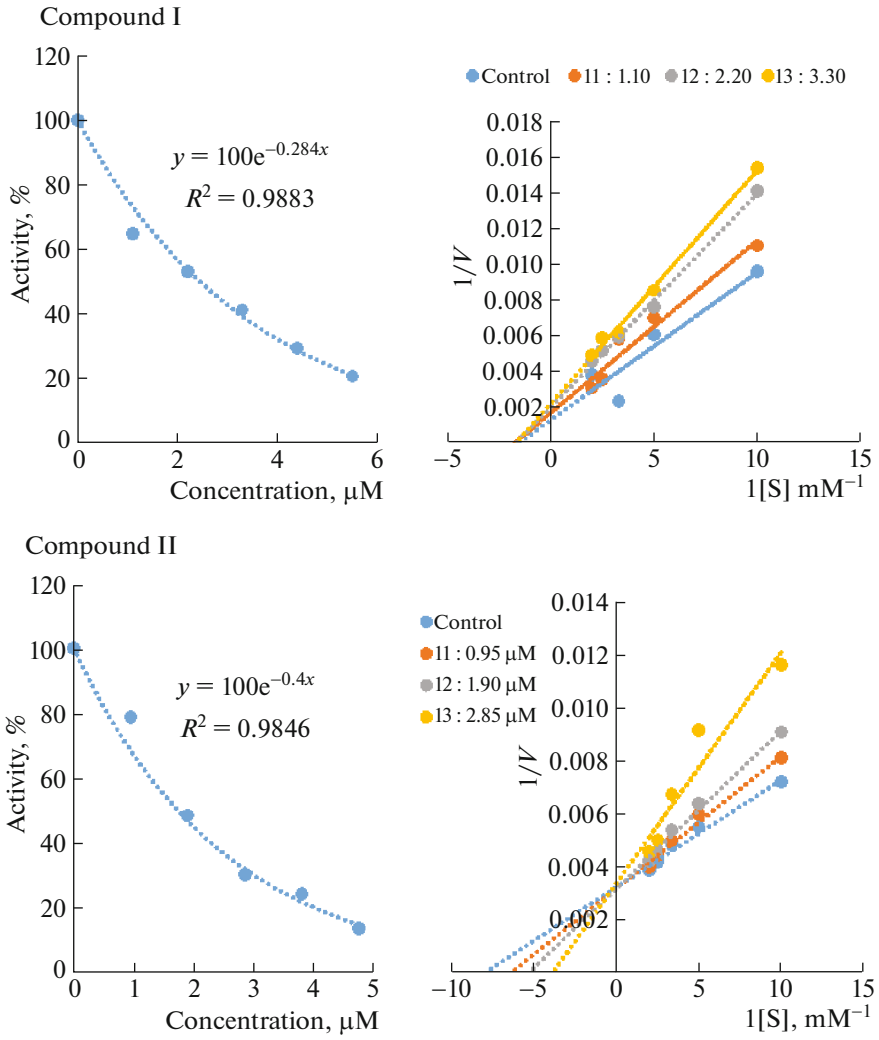

Fig. 2. Compounds (I, II) on AChE.

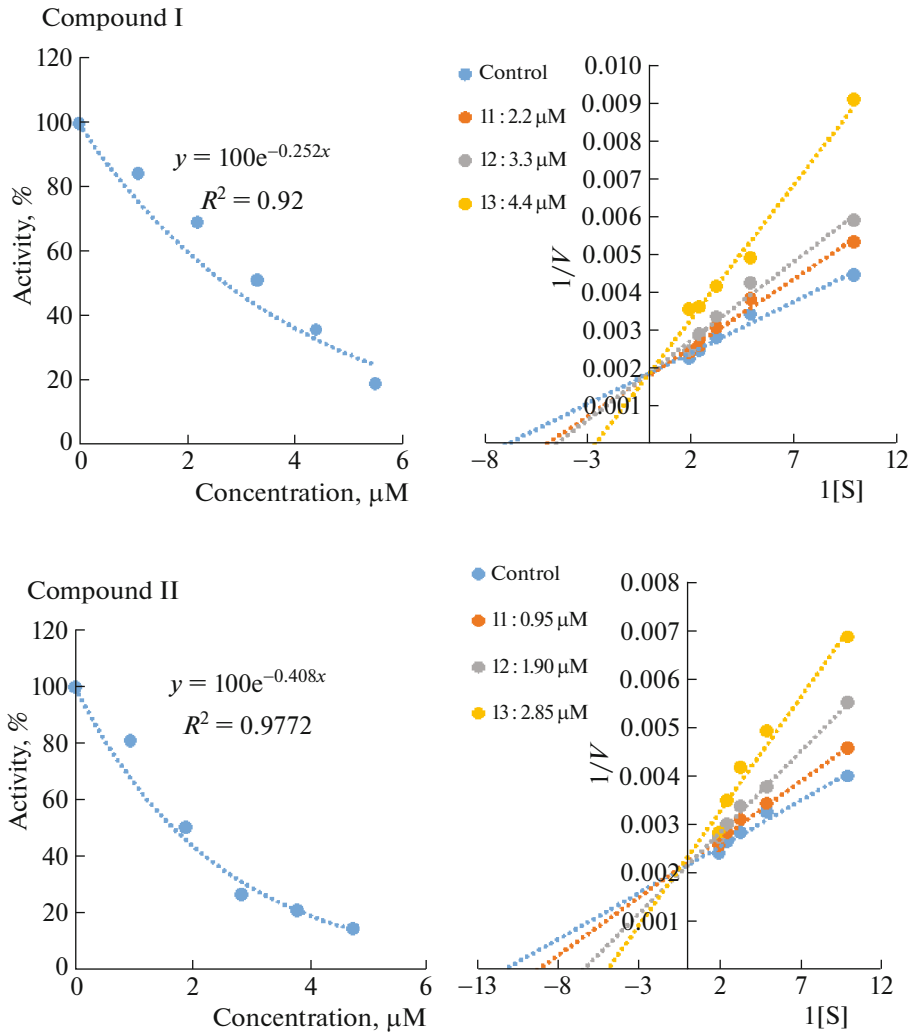

Fig. 3. Compounds (I, II) on GST.

compound I (−7.86 kcal/mol), indicating that compound II showed a strong affinity to GST. Compared with the reference co-crystal chlorambucil, the newly synthesized ligands showed higher binding affinity for receptor. When the interactions between compound II and GST are examined, it is seen that the ligand has formed two carbon hydrogen bonds, two pi-alkyl bonds, one alkyl bond, one pi-sigma bond and one pi-pi stacked bond, and two of these bonds have an atomic distance lower than 4 Å. The bond with the lowest atomic distance was in position Pro9 with the length of 3.46 Å. On the other hand, the compound I compound showed strong affinity for the target protein, similar to the compound II compound. The ligand compound I formed two conventional hydrogen bonds and two pi-alkyl bonds, and two of them have an atomic distance lower than 3 Å. The strongest bond of that interaction formed at position Tyr7 with a length of 2.72 Å. Additionally, profiling of protein-ligand interactions showed similar interacting key residues (Val19, Tyr7, and Arg13) at the active site of the receptor protein. The binding poses and interactions of ligands against receptor protein are presented in detail in Figs. 4 and 5.

Pharmacokinetics and ADME Prediction

ADME is an acronym that stands for absorption, distribution, metabolism, and excretion. These are the four processes that a drug undergoes in the body after it is administered. Generally, these parameters are used to evaluate potential interactions between drug and other non-drug target molecules [43–46]. In order for a compound to be used as a potential drug, it should obey the Lipinski rule of five. These are: (a) molecular weight <500 Daltons, (b) high lipophilicity (expressed as log*P* 5), (c) H-bond donor <5, (d) H-bond acceptor <10, (e) molar refractivity between 40 and 130. The SwissADME server was used to determine whether the two compounds used in the

Table 5. Summary of two newly synthesized compounds and reference molecule against glutathione s-transferase enzyme with the binding energies, numbers of hydrogen bonds, number of closest residues, and the interacting residues

Ligand name	Free binding energy, kcal/mol	Ki value	Number of HBs	Number of closest residues	Interacting key residues
II	−8.20	979.26 nM	2	Tyr108, Leu52, Gln51, Trp38, Asn204, Gly205	Tyr7, Phe8, Pro9, Val10, Arg13, Ile104, Pro202
I	−7.86	1.73 μM	2	Gly205, Phe8, Tyr108, Gly12, Ile104, Gln51, Pro53, Asn66, Glu97, Leu52, Ser65, Asn204	Tyr7, Val10, Arg13, Gln64
*Chlorambucil	−5.25	142.45 μM	5	Thr34, Ile104, Asn204	Tyr7, Phe8, Pro9, Val10, Gly12, Arg13, Val35, Trp38, Tyr108, Gly205

* Reference molecule.

Table 6. Pharmacokinetics and ADME properties of ligands docked with GST

Lipinski's rule of five									
ligand name	mol. weight	log*P*	H-bond donor	H-bond acceptor	molar refractivity	heavy atoms	aromatic heavy atoms	rotatable bonds	TPSA
Compound II	513.36	4.01	1	6	123.73	32	23	7	114.79 Å
Compound I	437.27	2.87	1	6	99.25	26	17	5	114.79 Å
ligand name	ESOL class	GI absorption	BBB permeant	Pgp substrate	bio availability Score	PAINS alerts	synthetic accessibility	violations	drug likeliness
Compound II	Mod. soluble	High	No	No	0.55	0	3.75	Yes, 1	Yes
Compound I	Mod. soluble	High	No	No	0.55	0	3.26	No	Yes

present study passed Lipinski's rule of five. The pharmacokinetic, physicochemical, and drug-like properties of the compounds were revealed (Table 6). The results revealed that the two compounds showed good drug-like properties based on Lipinski's rule of five, with additional parameters of drug likeness. Therefore, we propose that the two newly synthesized molecules I–II have the potential to work effectively as novel drugs.

EXPERIMENTAL

Synthesis of 1,2,4-Triazol 4-Bromobenzenesulfonates (I, II)

4-Formphenyl 4-bromobenzenesulfonate and 4-amino-5-methyl-2,4-dihydro-3*H*-1,2,4-triazol-3-one/ 4-amino-5-benzyl-2,4-d,hydro-3*H*-1,2,4-triazol-3-one were placed in the flask and mixed by controlled heating in the oil bath at 160–170°C. The reaction optimum conditions were determined by TLC. After 1 h, the reaction was closed and the contents of the flask were cooled. The precipitates were purified from ethyl alcohol-diethyl ether (1 : 3) (Scheme 1).

(E)-4-(((3-Methyl-5-oxo-1,5-dihydro-4H-1,2,4-triazol-4-yl) imino) methyl) Phenyl 4-bromo benzene sulfonate (I). 81.30%, m.p. 225–228°C. IR (KBr, cm^{-1}): 3177 (NH), 3048 (=CH), 2883 (–CH), 1698 (C=O), 1602 (C=N), 1573 (C=C); ^{1}H NMR (400 MHz, DMSO-d_6) δ: 2.27 (s, CH_3, 3H), benzene H [7.20 (d, 2H), 7.81–7.90 (m, 6H)], 9.72 (s, N=CH, 1H), 11.84 (s, NH, 1H); ^{13}C NMR (100 Hz, DMSO-d_6) δ: 10.93 (CH_3), benzene C [123.23 (2CH), 129.68 (2CH), 129.97 (C), 130.80 (2CH), 133.35 (C), 133.53 (2CH), 133.75 (C), 144.65 (C)], 150.95 (C=N triazol), 151.55 (C=O), 152.38 (N=CH).

(E)-4-(((3-benzyl-5-oxo-1,5-dihydro-4H-1,2,4-triazol-4-yl) imino) methyl) phenyl 4-bromo benzene sulfonate (II). 80.50%, m.p. 191–194°C. IR (KBr, cm^{-1}): 3169 (NH), 3031 (=CH), 2883 (–CH), 1703 (C=O), 1589 (C=N), 1574 (C=C); ^{1}H NMR

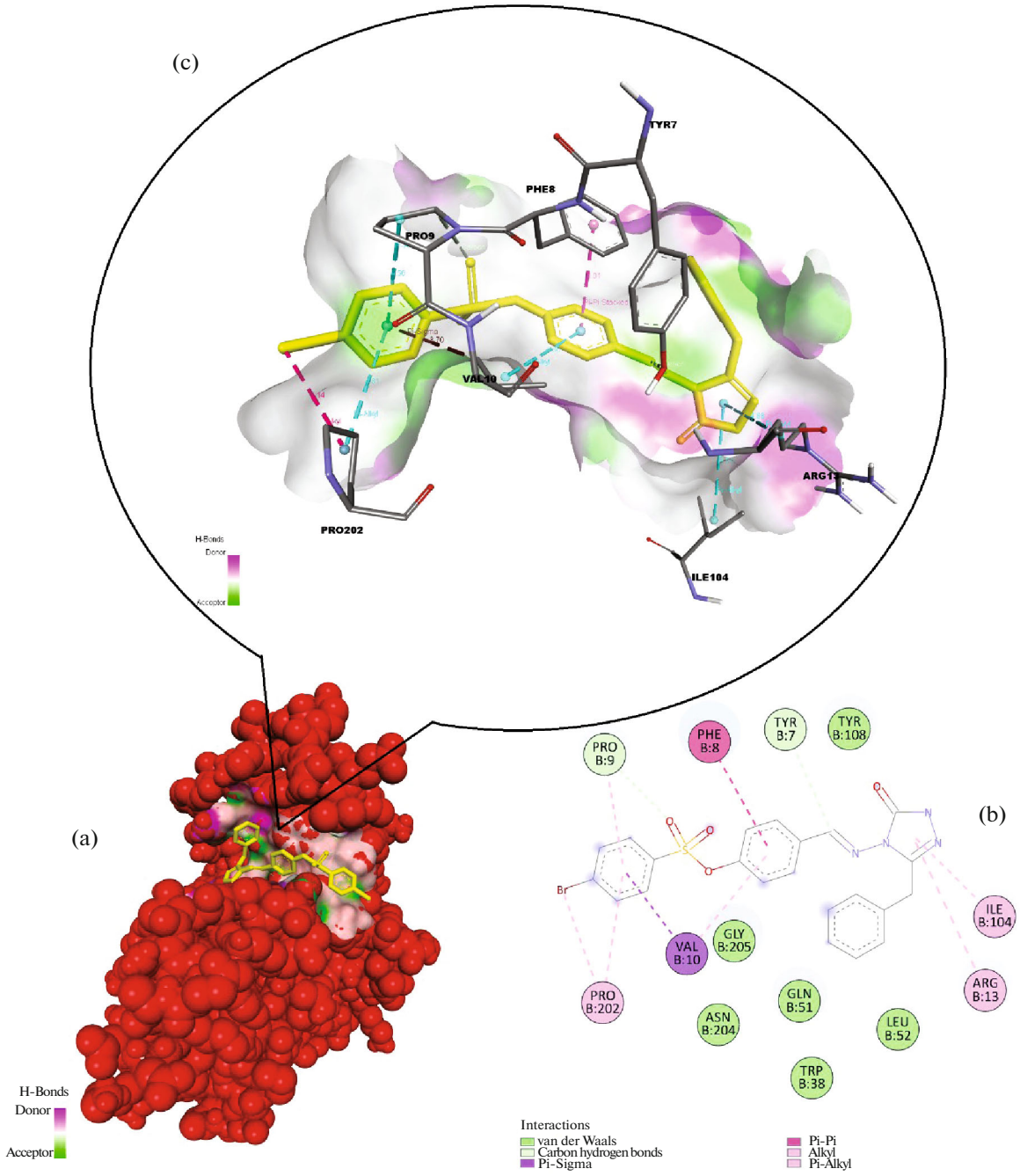

Fig. 4. Binding pose profile of benzyl at the active site of GST by BIOVIA Discovery Studio Visualizer (a), red shaped molecule represents the receptor and yellow shaped molecule indicates the ligand. 2D (b) and 3D (c) interaction analysis of GST with compound II.

(400 MHz, DMSO-d_6) δ: 2.27 (s, CH_3, 3H), benzene H [7.18–7.32 (m, 7H), 7.80–7.92 (m, 6H)], 9.68 (s, N=CH, 1H), 12.00 (s, NH, 1H); ^{13}C NMR (100 Hz, DMSO-d_6) δ: 31.07 (CH_2), benzene C [123.26 (2CH), 129.95 (2CH), 129.99 (C), 130.67 (2CH), 133.38 (C), 133.53 (2CH), 133.74 (C), 144.69 (C)], benzyl C [127.20 (CH), 128.92 (2CH), 129.26 (2CH), 136.21 (C)], 150.95 (C=N triazol), 151.59 (C=O), 152.14 (N=CH).

CONCLUSIONS

Compounds I, II were synthesized and characterized by FTIR and NMR spectroscopic methods. Density Functional Theory (DFT) method with 6-311++G(*d,p*) basis set was used for the theoretical study of compounds I and II. Optimized molecular structures and spectral parameters were obtained for compounds. Theoretical spectral data were compared

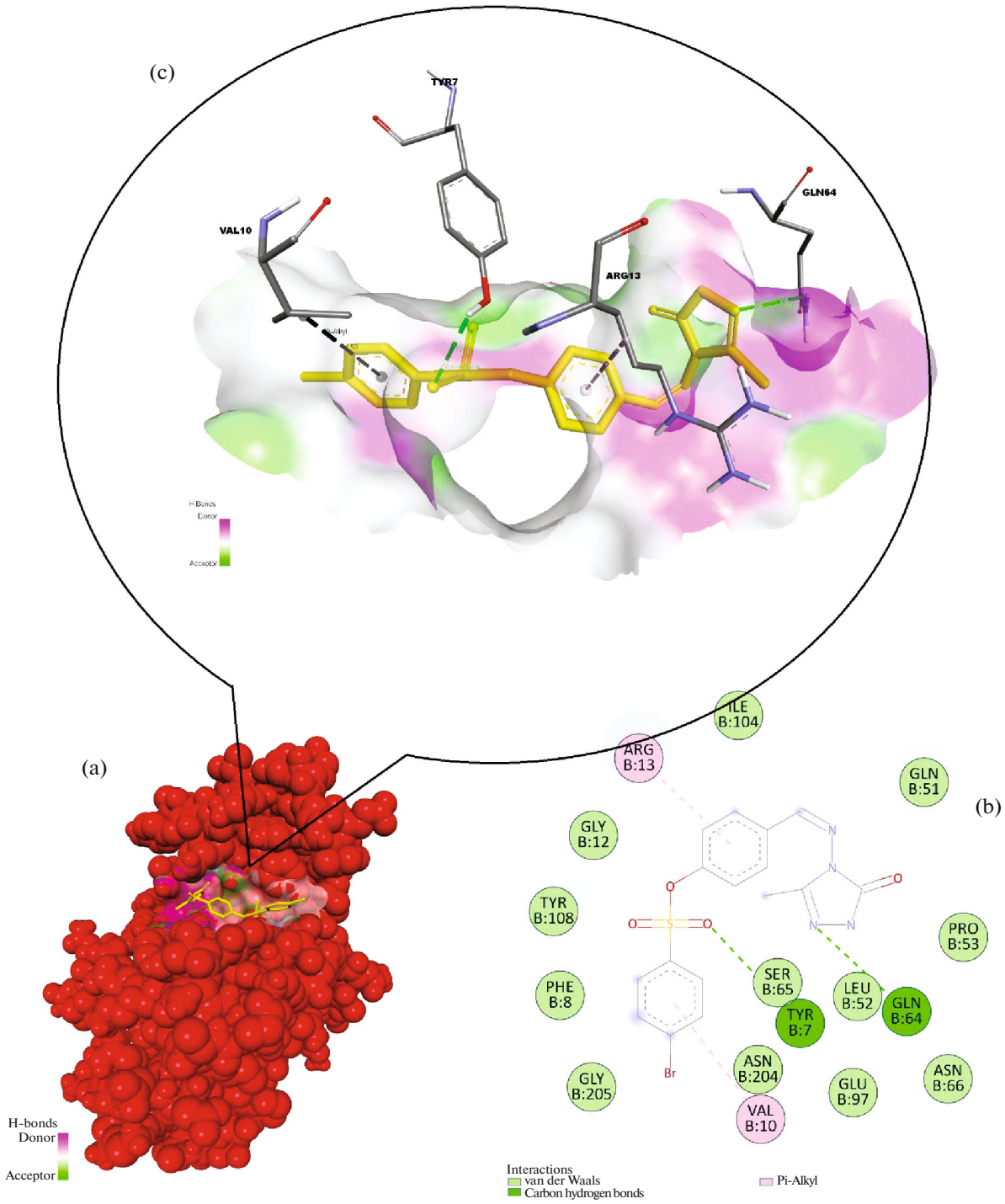

Fig. 5. Binding pose profile of metyl at the active site of GST by BIOVIA Discovery Studio Visualizer (a), red shaped molecule represents the receptor and yellow shaped molecule indicates the ligand. 2D (b) and 3D (c) interaction analysis of GST with compound I.

with experimental ones and the presence of intermolecular hydrogen bonds was evaluated. Results show that in the molecular structure of compounds are available N–H···O type strong intermolucular hydrogen bonds. The inhibition effects of compounds I, II on AChE and GST enzymes were investigated. When all the results are evaluated, it is seen that organic molecules have a weaker effect for the AChE enzyme than the standard. Looking at the results for the GST enzyme, it is seen that both molecules are more effec-

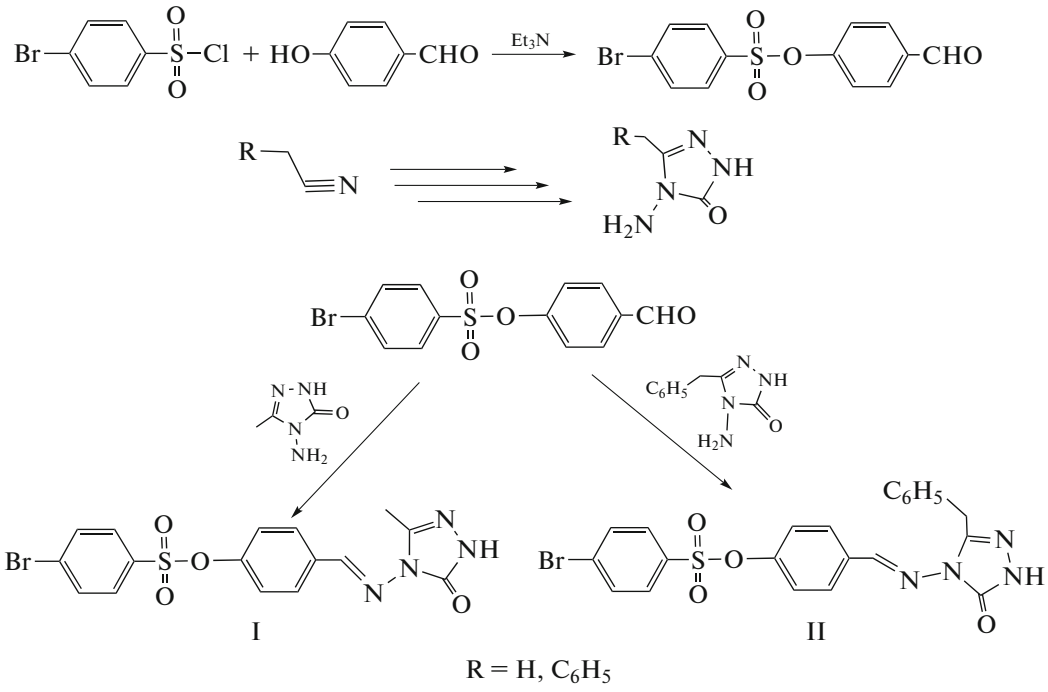

Scheme 1. Synthetic pathway for the preparation of compounds I and II.

tive than the standard. After examining the effects of these molecules on various cell lines, we can suggest that they can be marketed as drugs, supported by in vivo studies. In addition, The docking results showed that compounds I, II had appreciably strong binding affinities against glutathione s-transferase. Results of molecular docking including binding energies, compound II showed a higher docking score (−8.20 kcal/mol) with receptor protein compared to that of the other ligand compound I (−7.86 kcal/mol), indicating that compound II showed a strong affinity to GST. The SwissADME server was used to determine whether the two compounds used in the present study passed Lipinski's rule of five. The pharmacokinetic, physicochemical, and drug-like properties of the compounds were revealed. The results revealed that the two compounds showed good drug-like properties based on Lipinski's rule of five, with additional parameters of drug likeness. Therefore, we propose that the two newly synthesized molecules I, II have the potential to work effectively as novel drugs.

SUPPLEMENTARY INFORMATION

The online version contains supplementary material available at https://doi.org/10.1134/S0036024424040204.

ACKNOWLEDGMENTS

The numerical calculations reported in this paper were fully performed at TUBITAK ULAKBIM, High Performance and Grid Computing Center (TRUBA resources).

FUNDING

This work was supported by Karadeniz Technical University.

CONFLICT OF INTEREST

The authors of this work declare that they have no conflicts of interest.

REFERENCES

1. T. H. Lowry and K. S. Richardson, *Mechanism and Theory in Organic Chemistry,* 3rd ed. (Harper and Row, New York, 1987).
2. H. S. Tsai, J. J. Lin, W. F. Lien, and Y. Z. Wang, Appl. Polym. Sci. **116**, 1686 (2010).
3. K. Zhang, S. Fischer, M. Gruner, T. Groth, J. Helm, and D. Peschel, Polymer **51**, 4698 (2010).
4. P. Seedevi, M. Moovendhan, A. Shanmugam, and S. Vairamani, Int. J. Biol. Macromol. **99**, 519 (2017).
5. M. Tan, H. Wang, Y. Wang, G. Chen, L. Yuan, and H. Chen, J. Mater. Chem. B **2**, 569 (2014).
6. N. R. Pires, A. L. Angelim, P. L. Cunha, R. C. de Paula, J. P. Feitosa, J. S. Maciel, and V. M. Melo, Carbohydr. Polym. **91**, 92 (2013).
7. J. Yang, J. Cai, L. Chen, Y. Du, K. Luo, D. Li, and S. Yu, Int. J. Biol. Macromol. **52**, 25 (2013).
8. A. Jain, A. Gulbake, P. Hurkat, S. Shilpi, and S. K. Jain, Ther. Drug Carrier Syst. **30**, 91 (2013).
9. Y. Ünver, N. Süleymanoğlu, R. Ustabaş, H. İ. Güler, E. Bektaş, K. İ. Bektaş, and F. Çelik, J. Indian Chem. Soc. **99**, 100690 (2022).

10. L. Hariss, Z. Barakat, F. Fares, R. Gree, A. Hachem, and T. Roisnel, Tetrahedron Lett. **60**, 292 (2019).

11. S. S. Kumar and H. P. Kavitha, Mini-Rev. Org. Chem. **10**, 40 (2013).

12. C. G. de Oliveira, G. F. Andrade, M. F. Cabral, B. A. Cotrim, E. Delia, V. W. Faria, G. O. Resende, and F. C. Souza, Phosphor. Sulfur Silicon Relat. Elem. **190**, 1366 (2015).

13. Y. Ünver and E. Bektaş, Lett. Drug Des. Discov. **14**, 706 (2018).

14. R. Ustabas, N. Süleymanoğlu, H. Tanak, Y. B. Alpaslan, Y. Ünver, and K. Sancak, J. Mol. Struct. **984**, 137 (2010).

15. J. Nalawade, A. Shinde, A. Chavan, P. Choudhari, S. Patil, M. Suryavanshi, M. Modak, V. D. Bobade, and P. C. Mhaske, Eur. J. Med. Chem. **179**, 649 (2019).

16. X.-M. Chu, K.-K. Gong, L.-L. Liang, W. Liu, K.-L. Sun, C. Wang, and W.-L. Wang, Eur. J. Med. Chem. **166**, 206 (2019).

17. A. T. Shahzad Bale, M. Bajda, A. Mahmood, L. Shahzadi, M. Yar, Z. A. Khan, S. A. R. Naqvi, S. Ullah, A. J. Shaikh, T. A. Sherazi, and J. Kukulowicz, Bioorg. Chem. **85**, 209 (2019).

18. K. Sancak, Y. Ünver, H. Tanak, İ. Değirmencioğlu, E. Düğdü, M. Er, and Ş. Işık, J. Incl. Phenom. Macrocycl. Chem. **67**, 325–334 (2010).

19. K. S. Raju, V. S. Krishna, G. Sabitha, D. Sriram, S. R. Sagurthi, S. A. Reddy, and K. B. Reddy, Bioorg. Med. Chem. Lett. **29**, 284 (2019).

20. A. Sahu, R. K. Agrawal, D. Das, and A. Gajbhiye, Life Sci. **228**, 176 (2019).

21. V. Alagarsamy, K. Kavitha, S. Meena, M. Rupeshkumar, D. Shankar, A. A. Siddiqui, and R. Rajesh, Eur. J. Med. Chem. **43**, 2331 (2008).

22. K. Karrouchiac, M. Ansar, M. El Abbes Faouzi, L. Chemlal, Y. Cherrah, J. Taoufik, and S. Radi, Ann. Pharm. Fr. **74**, 431 (2016).

23. Y. Ünver, K. Sancak, F. Çelik, E. Birinci, M. Küçük, S. Soylu, and N. A. Burnaz, Eur. J. Med. Chem. **84**, 639 (2014).

24. Y. Ünver, S. Deniz, F. Çelik, Z. Akar, M. Küçük, and K. Sancak, J. Enzyme Inhib. Med. Chem. **31**, 89 (2016).

25. Q. Liu, R. Bai, J. Jiang, J. Liu, M. Shen, S. Xu, J. Xu, X. Yang, H. Zhang, and H. Yao, Bioorg. Med. Chem. **21**, 7742 (2013).

26. X. Cao, L. Bao, W. Wang, and S. Wang, Eur. J. Med. Chem. **139**, 718 (2017).

27. A. Kaur, B. Goyal, D. Goyal, S. Mann, N. Priyadarshi, and N. K. Singhal, Bioorg. Chem. **87**, 572 (2019).

28. N. Süleymanoglu, R. Ustabaş, S. Direkel, Y. B. Alpaslan, and Y. Ünver, J. Mol. Struct. **1150**, 82 (2017).

29. H. Medetalibeyoğlu, S. Manap, F. Türkan, and H. Yüksek, J. Biomol. Struct. Dyn. **20**, 1 (2022).

30. A. Aras, O. Akyıldırım, M. Beytur, S. Boy, H. S. Karaman, S. Manap, F. Türkan, and H. Yüksek, Chem. Biodivers. **18**, e2100433 (2021).

31. S. M. Abdalrazaq, M. S. Agırtaş, A. Aras, H. U. Celebioglu, Y. Erden, F. Turkan, P. Taslimi, B. Tuzun, and I. Gulçin, J. Biomol. Struct. Dyn. **39**, 3693 (2021).

32. M. N. Atalar, A. Aras, M. Ahmad, E. Bursal, M. A. Yılmaz, E. Izol, M. Murahari, and F. Türkan, Biophys. Chem. **277**, 106629 (2021).

33. A. Aygun, H. Şakiroğlu, F. Şen, and F. Türkan, BioNanoScience **9**, 683 (2019).

34. İ. Gulcin, H. S. Karaman, P. Taslimi, F. Türkan, K. Turhan, and Z. Turgut, J. Heterocycl. Chem. **57**, 3116 (2020).

35. N. Vembu and F. R. Fronczek, Acta Crystallogr., Sect. E **65**, o2681 (2009).

36. M. J. Guo, X. Chen, and J. Yao, Acta Crystallogr., Sect. E **66**, o1360 (2010).

37. U. Çoruh, R. Ustabaş, K. Sancak, S. Şaşmaz, E. Agar, and Y. Kim, Acta Crystallogr., Sect. E **59**, o1277 (2003).

38. I. Yılmaz, N. B. Arslan, C. Kazak, K. Sancak, and Y. Unver, Acta Crystallogr., Sect. E **62**, o3067 (2006).

39. A. Aras, N. Çolak, E. Bursal, K. Buldurun, M. Murahari, F. Turkan, N. Turan, and M. Yergeri, Biometals **34**, 393 (2021).

40. N. Balcı, E. Bursal, H. Şakiroğlu, and F. Türkan, J. Biomol. Struct. Dyn. **40**, 11587 (2022).

41. D. Chen, S. M. Dann, C. Ferguson, N. Oezguen, P. Urvil, and T. C. Savidge, Sci. Adv. **2**, e1501240 (2016).

42. C. A. Dowd, V. M. Foley, G. Meade, and D. Sheehan, Biochem. J. **360**, 1 (2001).

43. C. A. Lipinski, Drug Discov. Today Technol. **1**, 337 (2004). https://doi.org/10.1016/j.ddtec.2004.11.007

44. B. Jayaram, G. Mukherjee, A. Mathur, T. Singh, S. Shekhar, and V. Shekhar, BMC Bioinform. **13**, S7 (2012).

45. S. Das, S. Lyndem, S. Sarmah, and A. Singha Roy, J. Biomol. Struct. Dyn. **39**, 1 (2020).

46. L. Behera, R. Donde, G. Gouda, M. K. Gupta, S. Vemula, and R. Vadde, J. Biomol. Struct. **39**, 2617 (2020).